Laser Frequency Chirping With Silicon Photonic Circuit Comprising an IQ Modulator and a III-V/Si SOA

Martin Peyrou, F. Enault, F. Mazur, K. Froberger, Z. Yong, T. Thiessen, J. Mak, F. Denis-Le-Coarer, M. Marchenay, L. Milord, et al.

Laser Frequency Chirping with Silicon Photonic Circuit comprising an IQ Modulator and a III-V/Si SOA

M. Peyrou, F. Enault, F. Mazur, K. Froberger, Z. Yong, T. Thiessen, J. Mak, F. Denis-Le-Coarer, M. Marchenay, L. Milord, Y. Le Guennec, F. Moysan and S. Menezo

***Abstract*—We report on the performance of a silicon photonic integrated circuit for laser frequency chirping, developed for FMCW LIDAR applications. An external laser source is fiber coupled to the photonic circuit and frequency chirping is achieved with a silicon IQ modulator and a monolithically integrated III-V/Si semiconductor optical amplifier to compensate for IQ modulator losses. A chirp distortion of 1.8% over 5% to 95% of the chirp ramp period was measured with a delayed self-heterodyne interferometric method. The high chirp linearity of our circuit is confirmed by FMCW ranging measurements using 2-18 m long fiber delay lines. The resulting beat frequency follows a linear dependency with the fiber delay line length (R^2=0.999).**

***Index Terms*—FMCW LIDAR, chirp, IQ modulator, SOA, linearity, silicon photonics**

I. Introduction

THE recent advances in high precision 3D sensing systems integration on-chip are gaining interest for self-driving cars, robotics, consumer, and medical applications, owing to their reduced size, weight, power consumption and cost (SWaP-C). Light detection and ranging (LIDAR) produces 3D pointcloud with better angular resolution than radio detection and ranging (RADAR) due to the wavelength of operation. Compared to direct time-of-flight (DToF) approach, frequency modulated continuous wave (FMCW) LIDAR uses a coherent receiver that provides strong selectivity against background light and high sensitivity, making it suitable for long-range detection [1]. However, FMCW LIDAR requires narrow linewidth lasers and high chirp linearity to reach quantum limited operation. Narrow linewidth lasers ensure the coherence between the local oscillator (LO) and received (RX) signals over long operating ranges, preventing signal-to-noise ratio (SNR) degradation due to phase noise, while nonlinear distortion of the frequency chirp broadens the detected signal spectrum, degrading the SNR and resolution [2].

Chirping the FMCW LIDAR signal can be either achieved through direct laser modulation or by using an external modulator with a fixed laser frequency. Direct modulation suffers from the nonlinear relationship between optical frequency and injection current. To mitigate nonlinearities, resampling methods [3], iterative learning pre-distortion of the driving signal [4], optical phase locked loop (OPLL) [5], or engineering of the laser structure [6] can be used. However, these chirp linearization methods may add latency, complexity, and cost to the system. Another drawback of direct laser modulation is a degradation of the laser linewidth due to the unwanted intensity modulation [7]. External modulation is therefore preferable for solving the narrow linewidth and chirp linearity challenges independently. Sub-kHz linewidth lasers demonstrated in [8] could be combined with IQ modulator to produce high linearity frequency chirps. External modulation also offers flexibility in the transmitted signal as shown in [9], where a fibered IQ modulator generates two independent linear frequency chirps in the lower and upper side bands (LSB and USB) for simultaneous measurement of the target range and radial velocity, reducing the time allocated to each pixel. Nevertheless, IQ modulation comes with high loss as the modulation is made at the carrier suppression point. In [10], a fibered FMCW LIDAR comprising an IQ modulator followed by an Erbium doped fiber amplifier (EDFA) has been reported but the chirp linearity was not measured. In this paper, we report for the first time on a Silicon IQ modulator with a monolithically integrated III-V/Si semiconductor optical amplifier (SOA) to demonstrate highly linear chirp generation for FMCW LIDAR applications.

In the first part of this paper, we report on our Photonic Integrated Circuit (PIC) and its packaging with an external driver. The second part describes the chirp linearity characterization setup. Measurement results are discussed in the third part. The last section is dedicated to an alternative method for evaluating chirp linearity, based on FMCW LIDAR range measurements for different fiber delay line lengths.

II. Integration Platform And Photonic Package

Our PIC is composed of a Si based high speed IQ modulator and a III-V/Si SOA fabricated on the same platform. The IQ modulator consists of two nested Mach-Zehnder Modulators (MZM I and MZM Q) that are DC biased at the minimum

Martin Peyrou is with SCINTIL Photonics, 38040 Grenoble, and Université Grenoble Alpes, CNRS, Grenoble-INP, GIPSA-lab, 38400 Saint-Martin-d'Hères, France (e-mail: martin.peyrou@scintil-photonics.com).

Sylvie Menezo is with SCINTIL Photonics, 38040 Grenoble, France (e-mail: sylvie.menezo@scintil-photonics.com).

transmission point. A phase shift of $\pi/2$ is inserted between the two MZMs. Light is coupled in and out of the chip by a fiber array aligned to surface Grating Couplers (GCs) defined in the Si. Fig. 1(a) shows a schematic cross section of the integration platform [11] used to fabricate the PIC. The PIC was mounted on a thermoelectric cooler (TEC) to ensure stable temperature operation. An electronic control board, including RF drivers was developed to command the PIC. The motherboard is fed by a 12V power supply. Fig. 1(b) shows a picture of the fabricated package.

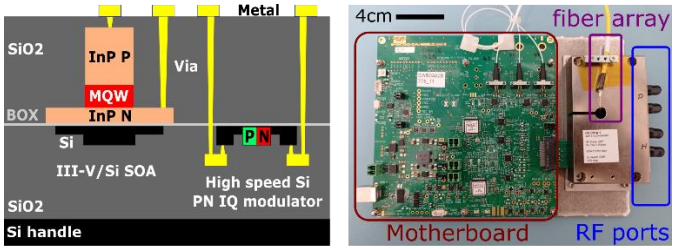

a) b)

Fig. 1. a) Schematic cross section of the integration platform b) picture of the PIC package with its motherboard.

III. IQ MODULATOR FREQUENCY CHIRP GENERATION

The schematic on Fig. 2 shows the working principle for FMCW LIDAR frequency synthesis in our circuit. An external laser having an optical power P_{las} =13dBm and an optical frequency f_{las} = 195.9THz (corresponding to a wavelength of 1530nm) feeds the on-chip IQ modulator and SOA. To produce the frequency chirp, a complex RF modulating signal u(t) is applied to the IQ modulator as:

$$u(t) = u_I(t) + ju_Q(t) \quad (1)$$

where $u_I(t)$ and $u_Q(t)$ are the RF signals applied to MZM I and MZM Q respectively.

To produce the $u_I(t)$ and $u_Q(t)$ RF signals, we used a 24GHz RADAR phase-locked loop (PLL) composed of a phase detector, a low pass filter and a voltage controlled oscillator (VCO) [12].

We performed triangular modulation composed of symmetric up- and down-ramps with period duration T of 154µs. The calculations are done for the signal under an up-ramp, while the same derivation applies to a down-ramp. Over an up-ramp period T, the PLL provides a RF output signal $s_R(t)$ given by:

$$s_r(t) \propto \cos(2\pi f_r t + \frac{\pi f_{exc}}{T} t^2) \quad (2)$$

where $s_r(t)$ describes an up linear frequency chirp starting at f_r = 24GHz with frequency excursion f_{exc}.

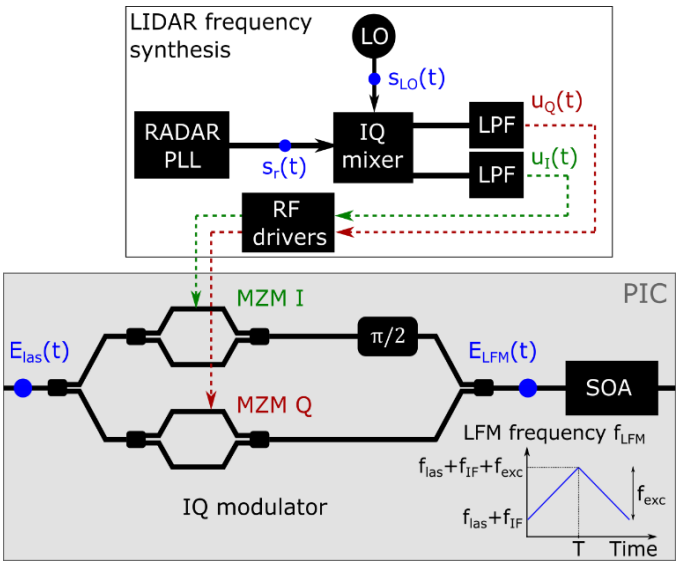

Fig. 2. Schematic of our FMCW LIDAR frequency synthesis scheme. The I and Q RF signals generation are applied to the PIC composed of an IQ modulator and III-V/Si SOA.

A local oscillator (LO) sine-wave $s_{LO}(t)$ ($f_{Lo} = 21.2GHz$) is generated as:

$$s_{LO}(t) \propto \cos(2\pi f_{LO} t) \quad (3)$$

$s_r(t)$ and $s_{LO}(t)$ are then mixed within the IQ mixer followed by Low Pass Filters (LPFs) to produce the $u_I(t)$ and $u_Q(t)$ signals [10]:

$$u_I(t) = \alpha_{RF} \cdot \cos(2\pi f_{IF} t + \frac{\pi f_{exc}}{T} t^2) \quad (4)$$

$$u_Q(t) = \alpha_{RF} \cdot \sin(2\pi f_{IF} t + \frac{\pi f_{exc}}{T} t^2), \quad (5)$$

where $f_{IF} = f_r - f_{LO}$ = 2.8GHz and α_{RF} is the amplitude of the RF signal.

The two RF signals are applied to the I and Q ports of the modulator to produce a Linear Frequency Modulation (LFM) with optical field, $E_{LFM}(t)$ given by:

$$E_{LFM}(t) \propto \mathrm{E_{las}}(t) \cdot \exp\left[j\left(2\pi f_{IF} t + \frac{\pi f_{exc}}{T} t^2\right)\right], \quad (6)$$

where $E_{las}(t)$ is the external laser field. The time domain evolution of the LFM frequency $f_{LFM}(t)$ is described on the insert of Fig 2. In our measurement, we produced a frequency excursion f_{exc} of 1.5 GHz.

The chirped signal is then amplified by a SOA biased at 120mA to produce a measured optical gain of G_{SOA} = 10dB.

IV. CHIRP LINEARITY MEASUREMENT RESULTS

Fig3 describes the chirp linearity measurement setup. It is based on delayed self-heterodyne interferometry (DSHI), where one arm of the interferometer is delayed so that the beat signal produced by the two interfering signals can be processed to assess the frequency chirp linearity [4]. We used a L = 2m fiber delay line corresponding to a delay time τ = 9.8ns in the first arm. In the other arm, a polarization controller was placed to match the polarization states of both arms.

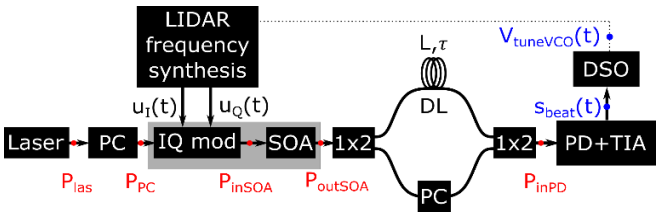

Fig. 3. Measurement setup to evaluate the chirp linearity from the IQ modulator. PC: polarization controller; SOA: semiconductor optical amplifier; DL: delay line; PD: photodiode; TIA: transimpedance amplifier; DSO: digital storage oscilloscope

The computed optical power budget of the measurement setup is described in Table I considering ideal splitters and lossless polarization controllers. We measured a 4.5dB loss per grating coupler, and the waveguide routing loss is 2dB. The IQ modulator insertion loss IL_{IQ} are computed from:

$$IL_{IQ} = 4 \cdot SL^4 \cdot EL \cdot \left(\frac{\pi}{2V_\pi}\right)^2 \alpha_{RF}^2, \quad (7)$$

where we note SL the splitter loss, EL the MZM excess loss, V_π the voltage to achieve π phase shift, and α_{RF} is the amplitude of the RF signals. A V_π of 6.5V was measured on each MZM with a delivered an amplitude α_{RF} of 2V. The MZMs are 3mm-long, and we measured a propagation loss due to the doped silicon of 2dB/mm, resulting in a MZM excess loss EL of 6dB. Considering ideal splitters (splitter loss SL of 3dB), the IQ modulator insertion loss is estimated around 18dB.

TABLE I: Computed optical power budget of the chirp linearity measurement setup.

Labels	Optical powers	Units
P_{las}	13	dBm
P_{PC}	13	dBm
P_{inSOA}	-11.5	dBm
P_{outSOA}	-1.5	dBm
P_{inPD}	-6	dBm

The PIC insertion loss can be reduced by 6dB using edge couplers (2dB loss per edge coupler) instead of grating couplers and silicon nitride (1dB loss) instead of silicon waveguides.

The beat signal $s_{beat}(t)$ is produced from the recombination of the two arms on an external photodiode. A transimpedance amplifier (TIA) with gain $G_{TIA} = 10V/A$ amplifies the photocurrent and converts it into a voltage. The beat signal is expressed by:

$$s_{beat}(t) \propto R \cdot P_{inPD} \cdot G_{TIA} \cdot \cos(2\pi f_{beat}(t)t) \quad (8)$$

where R is the photodiode responsivity (1A/W), P_{inPD} is the optical power at the photodiode input and $f_{beat}(t) = f_{LFM}(t) - f_{LFM}(t-\tau)$ is the beat signal frequency.

For $\tau \ll T$, the beat frequency can be approximated by its 1st order Taylor series expansion, i.e. $f_{beat}(t) \sim f_{LFM}{}'(t).\tau$. In our experiment, $\frac{\tau}{T} = \frac{1}{15306} \ll 1$, which validates this approximation.

The beat signal phase $\phi_{beat}(t)$ can then be extracted using a Hilbert transform (HT) over the ramp period T [3],[4]:

$$\phi_{beat}(t) = 2\pi\tau \int_T f_{LFM}{}'(t)dt = 2\pi\tau f_{LFM}(t) \quad (9)$$

The instantaneous frequency $f_{LFM}(t)$ is then obtained through:

$$f_{LFM}(t) = \frac{\Phi_{beat}(t)}{2\pi\tau} \quad (10)$$

Fig. 4(a) and (b) show the VCO command signal $V_{tuneVCO}(t)$ and the resulting time domain beat signal $s_{beat}(t)$ respectively, observed on a digital storage oscilloscope (DSO).

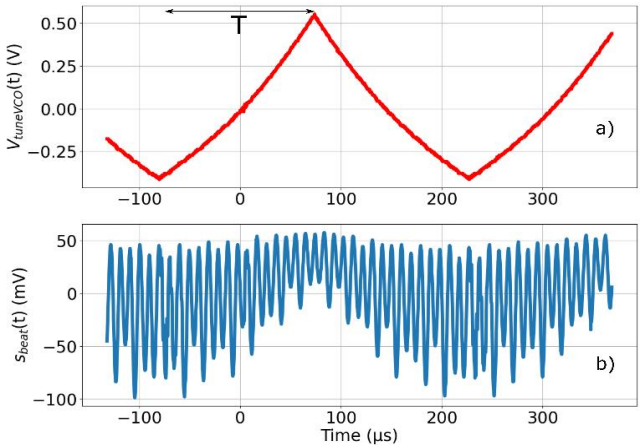

Fig. 4. Measured a) VCO command signal $V_{tuneVCO}(t)$ and b) time domain beat signal, $s_{beat}(t)$ on the DSO.

The $V_{tuneVCO}(t)$ curvature in Fig. 4(a) originates from the VCO nonlinearity compensation, ensuring linear frequency chirps at the PLL output.

We focus on the up-ramp of the frequency modulation for evaluating the linearity. Fig. 5(a) shows the instantaneous frequency retrieved from (9) and taken over 5%-95% of the up-ramp period T. The measured frequency excursion f_{exc} over this segment 1.38 GHz. The frequency chirp nonlinearity, as plotted on Fig. 5(b), is evaluated as the difference between the measured instantaneous optical frequency data and their best linear fit [6]. The superimposed curves on Fig. 5(b) correspond to 30 up-ramp periods. The standard deviation of the mean of these 30 curves is 24.3 MHz, which corresponds to 1.8% nonlinear distortion for a 1.38 GHz frequency excursion.

From Fig. 5(b), we noticed that the initial and final portion of the up-ramp are responsible for high nonlinearities. In these regions, the optical frequency undergoes sharp transitions. By considering 20%-80% of the chirp period T, the nonlinear distortion reduces to 0.4%. Iterative learning pre-distortion algorithms [4] could be used to reach a nonlinear distortion below 0.1%, as desired for automotive applications.

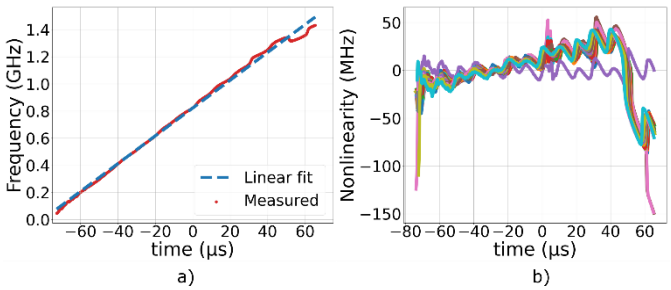

Fig. 5. a) Retrieved instantaneous frequency profile over 5%-95% of the up-ramp period T. b) Chirp nonlinearity obtained by subtracting the instantaneous frequency profile with a linear fit.

V. FMCW LIDAR RANGE MEASUREMENT RESULTS

FMCW LIDAR ranging measurements can be used as an alternative method for evaluating chirp nonlinearity, since the dependency between the beat frequency and the fiber length is linear for an applied linear frequency chirp. We performed these measurements for several fiber delay lengths (from 2-18m). For each fiber delay line, the polarization controller in the interferometer was adjusted to match the polarization state of the two arms. An estimate of the beat signal frequency is given by the maximum peak frequency of the Fast Fourier Transform (FFT) applied to the beat signal over 5%-95% of the period T. The measured spectra for each fiber length are superimposed on Fig. 6.

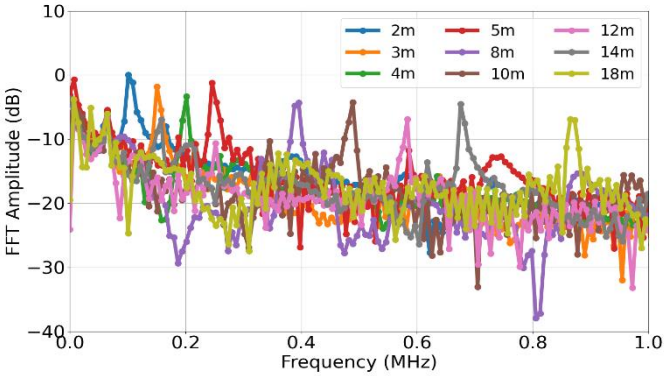

Fig. 6. Measured FFT spectra for several fiber lengths.

In Fig. 7, the measured beat frequencies are plotted against fiber length. We obtained a high linear coefficient of determination (R^2=0.999), confirming the chirp linearity measurement results. We measured the slope γ of the data plotted in Fig. 7, the frequency excursion f_{exc} can be obtained as:

$$f_{exc} = \gamma \frac{c}{n_g} T_{90\%}, \qquad (11)$$

where c is the speed of light in vacuum, n_g is the group index in the single mode fiber (1.4675 at 1550nm) and $T_{90\%}$ corresponds to the 5%-95% portion of the up-ramp period T, $T_{90\%} = 138\ \mu s$.

We measured a fitted slope γ of 48.2 kHz/m corresponding to a frequency excursion f_{exc} of 1.36GHz that matches the 1.38GHz frequency excursion measured in section IV. This translates into a range resolution of 11 cm [4].

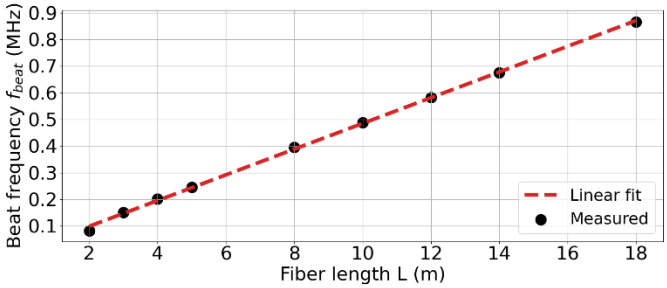

Fig. 7. Beat frequency against fiber length showing high linear dependency (R^2=0.999)

The measured chirping speed of 10 THz/s could be increased by reducing the ramp period T generated by the PLL. As a comparison in [5] and [6], the chirping speeds are 100 THz/s ($T = 1$ ms, $f_{exc} = 100$ GHz) and 90 THz/s ($T = 10\ \mu s$, $f_{exc} = 0.9$ GHz), respectively.

VI. CONCLUSION

In this paper, we reported on laser frequency chirping with a silicon photonic circuit integrating on the same chip a silicon IQ modulator and a III-V/Si SOA. The linearity of the generated chirp was measured and showed nonlinear distortion as low as 1.8% over 5% to 95% of the chirp period. These results were confirmed through range measurements with several fiber delay lines (2 to 18m) with good resolution. In the future, this PIC will be integrated with a coherent receiver to allow long range FMCW LIDAR operation.

ACKNOWLEDGMENT

The authors would like to acknowledge ANRT, the French BPI (Deeptech Program and ILAB contest) and the "Auvergne Rhône Alpes" region for their financial support.

REFERENCES

[1] B. Behroozpour, P. A. M. Sandborn, M. C. Wu and B. E. Boser, "Lidar System Architectures and Circuits," in IEEE Communications Magazine, vol. 55, no. 10, pp. 135-142, Oct. 2017.

[2] Qiao, L., Sun, D., Zhang, X. et al. Linearity Requirement for a Linear Frequency Modulation Lidar. OPT REV 6, 160–162 (1999).

[3] Tae-Jung Ahn, Ji Yong Lee, and Dug Young Kim, "Suppression of nonlinear frequency sweep in an optical frequency-domain reflectometer by use of Hilbert transformation," Appl. Opt. 44, 7630-7634 (2005).

[4] Xiaosheng Zhang, Jazz Pouls, and Ming C. Wu, "Laser frequency sweep linearization by iterative learning pre-distortion for FMCW LiDAR," Opt. Express 27, 9965-9974 (2019).

[5] Naresh Satyan, Arseny Vasilyev, George Rakuljic, Victor Leyva, and Amnon Yariv, "Precise control of broadband frequency chirps using optoelectronic feedback," Opt. Express 17, 15991-15999 (2009).

[6] S. Ayotte et al. "Narrow linewidth semiconductor DFB laser with linear frequency modulation for FMCW LiDAR," Proc. SPIE 11693, Photonic Instrumentation Engineering VIII, 116930F (5 March 2021).

[7] G. H. Duan and P. Gallion, "Drive current noise induced linewidth in tunable multielectrode lasers," in IEEE Photonics Technology Letters, vol. 3, no. 4, pp. 302-304, April 1991.

[8] Tran, M.A., Huang, D., & Bowers, J.E. Tutorial on narrow linewidth tunable semiconductor lasers using Si/III-V heterogeneous integration. *APL Photonics*. (2019).

[9] Shuang Gao, Maurice O'Sullivan, and Rongqing Hui, "Complex-optical-field lidar system for range and vector velocity measurement," Opt. Express 20, 25867-25875 (2012).

[10] S. Gao and R. Hui, "Frequency-modulated continuous-wave lidar using I/Q modulator for simplified heterodyne detection," Opt. Lett. 37, 2022-2024 (2012).

[11] S. Menezo et al. "40GBaud PAM4 silicon Mach-Zehnder modulator boosted by a heterogeneously integrated SOA with 10dB-gain," in *Optical Fiber Communication Conference (OFC) 2022*, paper Th3C.2.

[12] Goldman, Stanley. *Phase-Locked Loop Engineering Handbook for Integrated Circuits*, Artech House, 2007.